Barrier height at $(Ba,Sr)TiO_3$/Pt interfaces studied by photoemission

R. Schafranek,[1] S. Payan,[2] M. Maglione,[2] and A. Klein[1]
[1]*Darmstadt University of Technology, Institute of Materials Science, Petersenstrasse 23, D-64287 Darmstadt, Germany*
[2]*ICMCB-CNRS, Université Bordeaux 1, 87 Avenue, Dr. A. Schweitzer, Pessac 33608, France*
(Received 25 August 2007; revised manuscript received 13 April 2008; published 9 May 2008)

The interface formation of Nb-doped $SrTiO_3$ single crystals and $(Ba,Sr)TiO_3$ thin films with Pt has been studied by using photoelectron spectroscopy with *in situ* sample preparation. For the single crystal sample, a Schottky barrier height for electrons of 0.5–0.6 eV is determined after deposition of Pt in vacuum environment. After annealing in 0.05 Pa oxygen pressure, a strong increase in the barrier height to $\geq$1.2 eV is observed. X-ray induced photovoltages of up to 0.7 eV are observed in this case and have to be taken into account for a proper determination of the barrier height. A subsequent annealing in vacuum reduces the barrier again. Hence, the barrier height can be reversibly switched between an oxidized state with a large barrier height and a reduced state with a low barrier height. Quantitative analysis of the barrier heights indicates that the changes are related to the changes of interfacial defect concentration. Due to the occurrence of a Ti^{3+} related signal, the defects are identified as oxygen vacancies. The same effects are observed at interfaces between Pt and $(Ba,Sr)TiO_3$ thin films with a smaller absolute value of the barrier height in the oxidized state of $\sim$1 eV. Deposition of $(Ba,Sr)TiO_3$ onto a metallic Pt substrate also results in a barrier height of 1.0 eV.

DOI: 10.1103/PhysRevB.77.195310 PACS number(s): 73.30.+y, 79.60.Jv, 77.80.Fm

I. INTRODUCTION

$SrTiO_3$, $(Ba,Sr)TiO_3$, and $BaTiO_3$ (all abbreviated here as BST) are important materials for thin film electronic devices.[1–3] They are used, e.g., in metal-insulator-metal thin film capacitor stacks with Pt as a typical contact material. The choice of the metal electrode can have a considerable impact on the device behavior. This is at least partially related to the band gap of $SrTiO_3$ and $BaTiO_3$ of 3.2 eV,[4] which is rather small for an insulating material. Charge injection at the interface can therefore occur, in particular, if the barrier height at the interface is small. The metallic contact has, therefore, a strong impact on the leakage current behavior.[5,6] In addition, dielectric properties,[7] cycling stability,[8] and high frequency dielectric losses[9] are influenced by contact properties. The properties of the BST/Pt contact have already been extensively investigated by different techniques. Barrier heights can be derived, e.g., from electrical measurements including current-voltage, capacitance-voltage, and internal photoemission. A summary of barrier heights from such studies is given in Table I.

The Schottky barrier heights for electrons at BST/Pt contacts given in Table I considerably varies between Φ_B=0.4 and 1.6 eV. However, there seems to be a consistent trend in the experimental data depending on sample preparation. Interfaces prepared or treated under more reducing conditions result in a low barrier height ($\sim$0.4–0.7 eV) and interfaces prepared or treated in oxidizing conditions result in a larger barrier height ($\gtrsim$1.0 eV). A dependence of the barrier height on annealing conditions has been derived from electrical measurements.[6,11,17,18] However, the determination of barrier heights from electrical transport studies is not always unique due to the interdependence of parameters, the presence of more than one interface, and only partially known transport properties of the material itself. In addition, the microscopic origin for the variation in the barrier height cannot be accessed from transport studies, however.

An explanation for the variation of the barrier height was suggested by Dawber *et al.*[3,24] They emphasized the influence of the doping of the semiconductor on the barrier height, which can be treated by the model of Cowley and Sze[25] for semiconductor/metal interfaces. In this model, the dependence of barrier height on doping is related to the limitation of the potential drop in highly doped semiconductors.

Robertson and Chen[22] performed a theoretical calculation of the Schottky barrier height for various oxides based on the MIGS (metal-induced-gap-states) model. The calculation uses basic material and electronic structure parameters[26,27] and provides the charge neutrality level ϕ_0 and density of interface states. These are used as input for a calculation of the barrier height by using the formula given by Cowley and Sze[25] [see Eq. (3) below]. By using an electron affinity for $SrTiO_3$ of χ=3.9 eV and a Pt work function of ϕ_m=5.3 eV, Robertson and Chen[22] derived a Schottky barrier height of 0.89 eV.

Rao *et al.*[23] derived a rather large Schottky barrier height for electrons at the $BaTiO_3$/Pt interface. Their density functional theory calculation reveals a Fermi level position of 0.96 eV above the valence band maximum, which corresponds to the given barrier height for electrons Φ_B=2.19 eV for a $BaTiO_3$ energy gap of E_g=3.13 eV. However, the calculation yields an energy gap for $BaTiO_3$ of only $\sim$1.2 eV,[23] which is a well known limitation of density functional theory. Different scaling procedures can be applied to find the energy levels with respect to the experimental band gaps.[28] A shift of the conduction band edge is only one possibility to account for the differences in the calculated and experimental energy gaps.

Photoelectron spectroscopy has been widely used for many years to study semiconductor/metal interface formation.[29] This technique provides simultaneous information on electronic and chemical properties of the interfaces. It is therefore particularly suitable to identify the basic mechanisms of barrier formation. Although a number of such studies are available for BST/Pt interfaces,[20,21,30–33] the depen-

 ©2008 The American Physical Society

Urheberrechtlich geschützt / In Copyright

TABLE I. Schottky barrier heights for electrons at differently prepared BST/Pt interfaces reported in literature. sc, single crystal $SrTiO_3$; epi, epitaxial thin film; *p*, polycrystalline thin film; *c*, sintered ceramic; *IV*, current-voltage; *CV*, capacitance-voltage; PES, photoemission; dep, as-deposited metal contact; ann, contact annealed without specified atmosphere; H_2, contact annealed in hydrogen containing atmosphere; N_2, contact annealed in nitrogen; and O_2, contact annealed or prepared in oxygen containing atmosphere (including air).

Material	Φ_B/eV	Technique	Treatment	Ref.
p-$SrTiO_3$	1.1	*IV*		5
p-$(Ba,Sr)TiO_3$	1.0–1.2	*IV*	ann	10
p-$(Ba,Sr)TiO_3$	1.4	*IV*	O_2	11
epi-$SrTiO_3$	1.04	*IV*, *CV*	O_2	12
p-$(Ba,Sr)TiO_3$	0.51–0.73	*IV*, *CV*	dep	13
p-$(Ba,Sr)TiO_3$	1.05–1.27	*IV*	O_2	14
p-$(Ba,Sr)TiO_3$	1.5–1.6	*IV*, *CV*	N_2	15
p-$SrTiO_3$	0.9–1.3	*IV*	dep	16
p-$(Ba,Sr)TiO_3$	0.67/1.29	*IV*	dep/O_2	6
p-$(Ba,Sr)TiO_3$	0.6/1.0	*IV*, *CV*	H_2/O_2	17
p-$(Ba,Sr)TiO_3$	0.67/1.05	*IV*	dep/O_2	18
c-$BaTiO_3$	0.59/0.9–1.2	*IV*, *CV*	dep/O_2	19
sc-$SrTiO_3$	0.6	PES	dep	20
sc-$SrTiO_3$	0.4	PES	dep	21
sc-$SrTiO_3$	0.89	Theory		22
sc-$BaTiO_3$	2.19	Theory		23

dence of the barrier height on the interface preparation has not been addressed yet.

Chung *et al.*[21] studied the charge transfer interactions at interfaces between $SrTiO_3(100)$ and Pt by using Auger, x-ray, and UV photoelectron spectroscopies. A clean surface of the crystals was prepared by argon ion sputtering, which resulted in a highly reduced surface, as indicated by a considerable fraction of Ti^{3+} related emissions. Pt was evaporated by using a resistively heated W wire, resulting in a Schottky barrier height for electrons of $\Phi_B = 0.4$ eV.

A detailed photoemission study on the barrier formation at the $SrTiO_3$/Pt interface was reported by Copel *et al.*[20] They used $SrTiO_3$ single crystals with a (100) surface orientation and 0.05 and 0.5 wt % Nb concentrations. The surfaces were cleaned by heating in vacuum and 0.1 Pa oxygen pressure, resulting in a stoichiometric surface without evidence for Ti^{3+} species. Pt was stepwise evaporated by electron beam evaporation without breaking vacuum. A Schottky barrier height of 0.55–0.65 eV is reported.

Wang and McIntyre[30] deposited Pt by ion sputtering onto $Ba_{0.7}Sr_{0.3}TiO_3$ thin films prepared by metal-organic chemical vapor deposition. Pt deposition induced a band bending of ~0.4 eV, which is of the same magnitude as those determined by other authors[20,21,34] and also in this study. However, without knowledge of the initial band edge position with respect to the Fermi energy, this cannot be translated into a barrier height.

Recently Psiuk *et al.*[33] reported chemical changes in single crystal $SrTiO_3$ surfaces upon *ex situ* Pt deposition by electron-beam evaporation and magnetron sputtering. A considerable broadening of the Sr and Ti substrate emission lines and changes in surface composition are observed, particularly when Pt is deposited by magnetron sputtering. The changes are related to local heating of the substrate during deposition.

In this work, the barrier formation at BST/Pt interfaces is studied by using photoelectron spectroscopy. Surface preparation, thin film BST and Pt deposition, sample annealing, and analysis were all carried out in the same vacuum system (*in situ*), thereby avoiding surface contamination during the complete experiments. Particular emphasis will be given to the variation in the barrier height upon sample treatment and its origin. We will focus on the evaluation of the barrier formation of single crystal $SrTiO_3$. For comparison, the barrier formation of Pt with polycrystalline sputter deposited $Ba_{0.6}Sr_{0.4}TiO_3$ thin films is also presented. With these materials, the barrier formation can also be studied for the reverse deposition sequence, i.e., during deposition of BST onto Pt.

II. EXPERIMENT

The experiments were performed at the DArmstadt Integrated SYstem for MATerial research (DAISY-MAT), which combines a Physical Electronics PHI 5700 multitechnique surface analysis system with several deposition chambers by using an ultrahigh vacuum sample transfer.[35] X-ray photoelectron spectra were recorded by using monochromatic Al $K\alpha$ radiation with an energy resolution of ~0.4 eV, as determined from the Gaussian broadening of the Fermi edge of a sputter cleaned Ag sample.

Single crystal, (100)-oriented $SrTiO_3$ samples with dimensions of $10\times5\times1$ mm^3 purchased from CrysTec have been used in this study. For surface cleaning, the crystals were heated for 30 min to 650 °C in 0.05 Pa oxygen pressure for cleaning. The crystals were *n*-type doped with Nb (0.05 wt %=$1.7\cdot10^{19}$ cm^{-3}). Assuming an electron concentration equal to the Nb concentration and an electron mobility of 5 cm^2/Vs,[36–38] this corresponds to a conductivity of ~5 S/cm. We have determined the conductivity of our samples by using sputter deposited Pt contacts in a linear four-point probe geometry and obtained 1.3 S/cm, which is of the same order of magnitude.

$(Ba,Sr)TiO_3$ thin films were deposited by using radio frequency magnetron sputtering with a substrate temperature of 650 °C, a power density of 2.5 W/cm^2, a gas pressure of 5 Pa (99% Ar and 1% O_2), and a substrate to target distance of 9 cm. The deposition conditions are optimized to give a stoichiometric composition of the $(Ba,Sr)TiO_3$ films, as verified from quantitative x-ray photoelectron spectroscopy (XPS) and Rutherford backscattering spectroscopy.[39] The growth rate of the $(Ba,Sr)TiO_3$ film under these conditions is ~1.4 nm/min. The $(Ba,Sr)TiO_3$ films were deposited onto $SiO_2/TiO_2/Pt$ coated Si wafers purchased from INOSTEK.

Pt was deposited by dc-magnetron sputtering by using a metallic Pt target of 2 in. diameter, a power of 5 W, Ar gas pressure of 0.5 Pa, and a substrate to target distance of 10 cm. The base pressure in the sputter deposition chamber was 10^{-5} Pa. With these conditions, the growth rate of the Pt is ~2.8 nm/min.

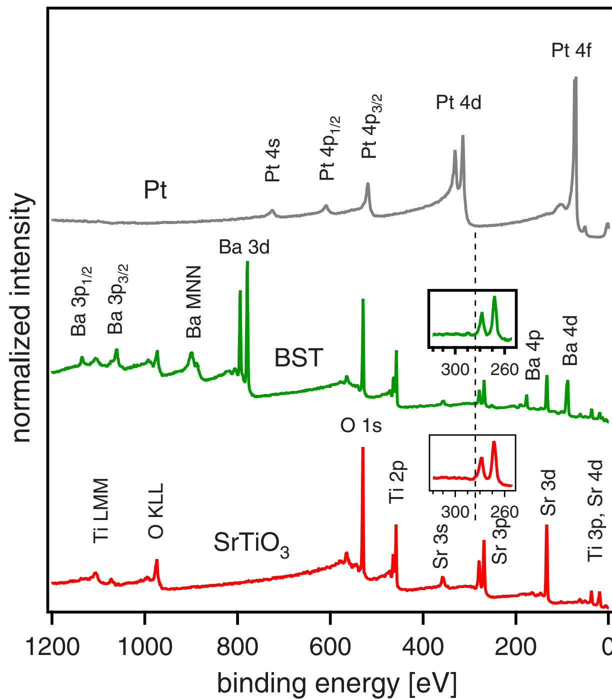

FIG. 1. (Color online) XPS survey spectra recorded with monochromatic Al $K\alpha$ radiation of a $SrTiO_3$Nb single crystal annealed in a 0.05 Pa oxygen pressure at 650 °C for 30 min, of a $Ba_{0.6}Sr_{0.4}TiO_3$ (BST) thin film of ~200 nm thickness, and of a thin Pt film of ~7.5 nm thickness. The dashed line indicates the position where C 1*s* emissions should be observed. The insets show magnified views of the binding energy region around the Sr 3*p* emission line in order to emphasize the absence of carbon.

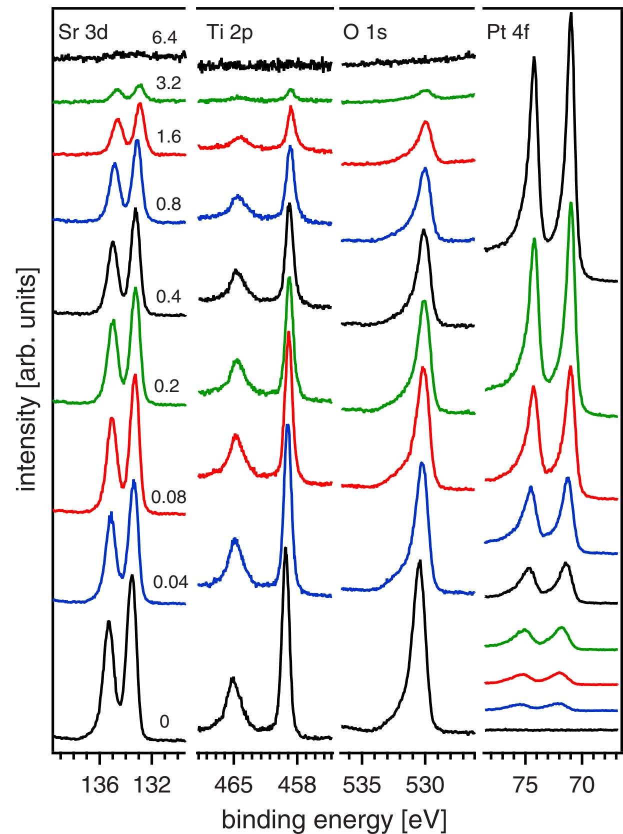

FIG. 2. (Color online) X-ray photoelectron spectra of a $SrTiO_3$:Nb(100) single crystal surface in the course of Pt deposition. The Pt film thickness is indicated in nm. All of the spectra were recorded by using monochromatic Al $K\alpha$ radiation and referenced to the Fermi edge of a sputter cleaned Ag sample.

To investigate the effect of annealing on the barrier height, ~2 nm of Pt was deposited onto freshly prepared surfaces. Subsequently, the sample was heated in an oxygen pressure of 0.05 Pa at 400 °C for 30 min. At last, the samples were heated in vacuum (10^{-5} Pa), again at 400 °C for 30 min. After each step, the samples were analyzed by using XPS and UV photoelectron spectroscopy (UPS). The complete preparation and analysis sequences were performed without breaking vacuum. No contaminations were observed after any step, which is justified from XPS survey spectra, as those shown in Fig. 1. The $SrTiO_3$:Nb and $Ba_{0.6}Sr_{0.4}TiO_3$ samples show only emissions of Sr, Ba, Ti, and O, indicating the absence of the typical hydrocarbon contaminations from the surface. All of the features observed from the Pt film after a deposition time of 160 s can be attributed to Pt emissions, also indicating an oxygen and carbon free surface. The work functions of $SrTiO_3$:Nb, $Ba_{0.6}Sr_{0.4}TiO_3$, and Pt as determined from UPS (not presented here) are 4.3, 4.3, and 5.5 eV, respectively, which are in good agreement with literature.[21,40–42]

III. BST/Pt INTERFACE FORMATION

A. Deposition of Pt onto $SrTiO_3$:Nb(100)

The valence band spectra of the annealed $SrTiO_3$:Nb single crystal recorded by using monochromated Al $K\alpha$ (see Fig. 7) and He I radiation (not shown here) are identical to those previously reported[40] and in good agreement with literature.[20,24,41] The valence band maxima (VBM) of the spectra are determined by linear extrapolation of the leading edge. Their binding energy with respect to the Fermi energy, which is calibrated as the zero of the binding energy scale, is given by $E_F - E_{VB} = 3.25 \pm 0.05$ eV, which is again in good agreement with previous values.[40] As the band gap of $SrTiO_3$ amounts to $E_g = 3.2$ eV,[4] this value corresponds to a Fermi level position at the conduction band minimum. Such a Fermi level position has to be expected for the given Nb doping level (see the discussion in Sec. IV C) and indicates that the surface Fermi level derived from the spectra is at the same position as in the bulk of the material (flat band condition).

To determine the Schottky barrier height of the $SrTiO_3$/Pt interface, Pt is stepwise deposited onto the clean $SrTiO_3$:Nb surface. After each deposition step, a full set of photoelectron spectra is recorded. Since the experimental setup allows for a fast sample transfer from the deposition chamber to the electron spectrometer in only a few minutes, such experiments can be performed within a single day, thereby avoiding surface contamination by long storage and transfer times.

Figure 2 shows the evolution of the substrate and overlayer core levels as a function of film thickness. A gradual attenuation of the substrate core levels and a corresponding

increase in the Pt emission is observed. The attenuation of the substrate signals corresponds well with a layer-by-layer growth mode of the Pt film, which is also verified by atomic force microscopy and which is in good agreement with the calculated high binding energies of Pt on $SrTiO_3$ and $BaTiO_3$ surfaces.[23,43]

Except for a small shoulder on the low binding energy side of the Ti 2*p* emission (see also the discussion in Sec. V), no significant change in the line shapes and half widths of the substrate emissions are observed during Pt deposition. This indicates a largely nonreactive interface.

The binding energy of the Pt 4*f* emission after the final deposition step is 71.0 ± 0.05 eV, which corresponds well with literature values for metallic Pt.[44] Also, the Fermi edge emission of the Pt film (see Fig. 7) coincides with the independently calibrated zero of the binding energy scale. At low coverage, the Pt 4*f* emission has a binding energy of up to 71.9 ± 0.1 eV, which is considerably larger than for the thick film. Such a behavior is frequently observed in this kind of experiments and typically explained by incomplete screening of the core hole in small metal islands (see, e.g., Ref. 45). In addition, the electronic structure of a single layer of Pt is significantly different from a thick Pt film due to the interaction with the substrate.[23,43] This will also contribute to the different binding energies of the Pt emissions at low coverage.

B. Deposition of Pt onto (Ba,Sr)TiO_3

Photoelectron spectra recorded during stepwise deposition of Pt onto $Ba_{0.6}Sr_{0.4}TiO_3$ are shown in Fig. 3. $Ba_{0.6}Sr_{0.4}TiO_3$ was deposited with a thickness of ~200 nm onto a $Si/SiO_2/TiO_2/Pt$ wafer at the beginning of the experiment by using the conditions described above. With increasing Pt deposition, the substrate core levels are gradually attenuated and the Pt emission intensity increases. All of the substrate emissions exponentially decay with decay constants corresponding to the inelastic mean free path of the individual lines. This indicates a layer-by-layer growth mode of Pt as also observed during deposition of Pt onto single crystal $SrTiO_3$ surfaces. As for the single crystalline substrate, no pronounced changes of the core level line shape are observed during Pt deposition.

The O 1*s* peak of the (Ba,Sr)TiO_3 film exhibits a shoulder on the high binding energy side. The O 1*s* emission of the $SrTiO_3$ single crystal also shows a noticeable asymmetry. Such features are often attributed to hydroxide species.[44] The oxygen shoulder on $SrTiO_3$ single crystals is particularly pronounced for the (100) surface orientation. A much weaker asymmetry is observed on the (110) and (111) orientations of identically prepared samples.[46] In addition, when preparing (Ba,Sr)TiO_3 thin films with a reduced distance between the sputter target and the substrate, no shoulder in the O 1*s* peak is observed (see the dotted spectrum in Fig. 3). Deposition under these conditions, which has a similar effect than a reduced gas pressure, leads to a nonstoichiometric sample composition with an ~20% Ti excess.[39] The barrier heights for both interfaces is, however, identical (see Sec. III D). The presence or absence of the O 1*s* shoulder therefore does not seem to affect the barrier heights.

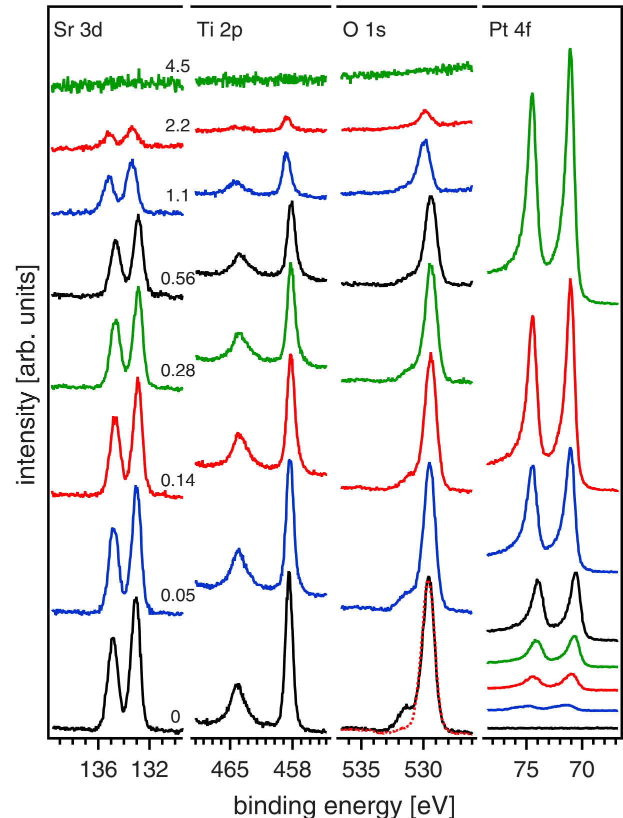

FIG. 3. (Color online) X-ray photoelectron spectra recorded during stepwise deposition of Pt onto $Ba_{0.6}Sr_{0.4}TiO_3$. The Pt film thickness is indicated in nanometers. All of the spectra were recorded by using monochromatic Al $K\alpha$ radiation and referenced to the Fermi edge of a sputter cleaned Ag sample. The O 1*s* spectrum of a BST film deposited under conditions which lead to a Ti excess is given as a dotted line.

Changes in barrier heights in semiconductor/metal hydrogen gas sensors have been attributed to the presence or absence of hydrogen at the interface.[47] Although we cannot fully exclude the contribution of hydrogen, we will provide evidence that oxygen vacancies are responsible for changes in the barrier height at the BST/Pt interface (see Sec. V).

C. Deposition of (Ba,Sr)TiO_3 onto Pt

As a substrate for the interface experiment to determine the barrier height, an INOSTEK wafer has been used. Prior to the first $Ba_{0.6}Sr_{0.4}TiO_3$ deposition step, the $Si/SiO_2/TiO_2/Pt$ substrate was annealed in the deposition chamber for 30 min at a temperature of 650 °C in the deposition atmosphere (total gas pressure of 5 Pa; 99% Ar and 1% O_2). After annealing, the sample was characterized by XPS, which revealed a clean substrate surface, as evident from the absence of carbon emissions. However, a small oxygen emission is observed after the heating step (see the bottom O 1*s* spectra in Fig. 4). This can be attributed to chemisorbed oxygen. Only a single Pt doublet with the asymmetric shape and binding energy of 71.0 eV typical for metallic platinum is observed in the Pt 4*f* spectrum of the substrate.[44]

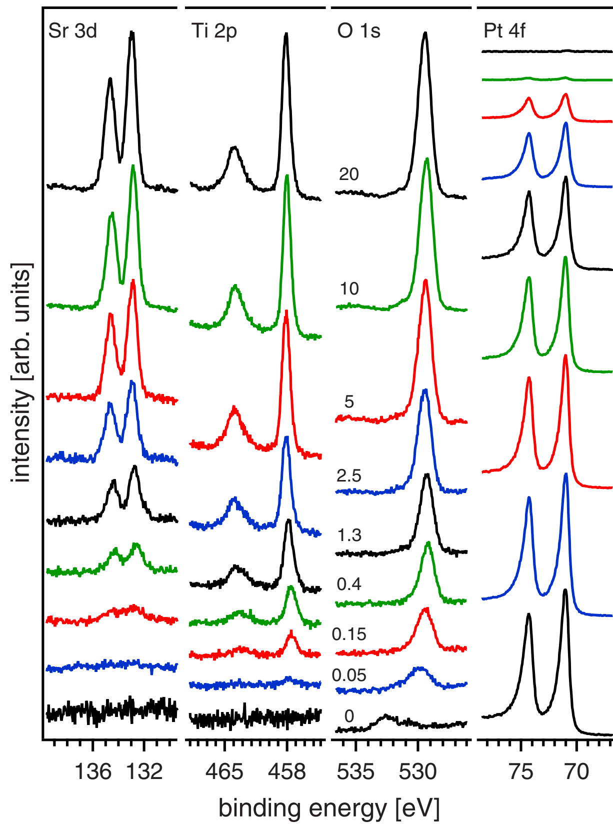

FIG. 4. (Color online) X-ray photoelectron spectra recorded during stepwise deposition of $Ba_{0.6}Sr_{0.4}TiO_3$ onto Pt. The substrate temperature during BST deposition was 650 °C. The film thickness is indicated in nm. All of the spectra were recorded by using monochromatic Al $K\alpha$ radiation and referenced to the Fermi edge of a sputter cleaned Ag sample.

For interface formation, the $(Ba,Sr)TiO_3$ films are prepared by using the conditions described above. Before each deposition, the sample was heated in the deposition atmosphere for half an hour in order to reach the desired deposition temperature of 650 °C. At the beginning of the sample heating, the plasma was started with a closed shutter in order to clean the target surface. To deposit the $(Ba,Sr)TiO_3$ film, after opening the shutter, the sample was rotated from the opposite position in the chamber under the target and held for the desired deposition time. Then, it was rotated back to the opposite side in the chamber, the shutter was closed and the plasma and heater power supplies were turned off. The sample was stored in the deposition chamber for cooling. After ~30 min, when the sample has cooled to below 150 °C, the gas supplies were closed and the sample was transferred to the XPS analysis chamber.

The described procedure allows for an accurate control of the $(Ba,Sr)TiO_3$ film thickness in the (sub)monolayer regime. With increasing deposition time, the BST emissions gradually increase and the Pt emission intensity is attenuated due to the increase in the BST layer thickness. The Pt 4f intensity exhibits an exponential decay with an attenuation only slightly slower than expected for a layer-by-layer-like growth mode of the film, indicating no pronounced island formation. The increase in the emission intensities of the

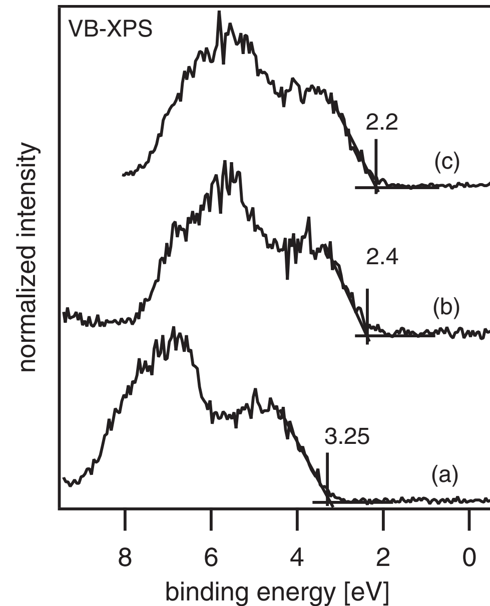

FIG. 5. X-ray valence spectra recorded from (a) $SrTiO_3$:Nb(100), (b) the ~200 nm thick $Ba_{0.6}Sr_{0.4}TiO_3$ film used as substrate for Pt deposition, and (c) ~20 nm thick $Ba_{0.6}Sr_{0.4}TiO_3$ film stepwise deposited onto Pt. All of the spectra were recorded by using monochromatic Al $K\alpha$ radiation and referenced to the Fermi edge of a sputter cleaned Ag sample. The determination and position of the valence band maxima are indicated.

BST film is almost parallel. The small differences can be related to the different kinetic energies of the photoelectrons, which result in different inelastic mean free paths.

No pronounced change in the shape of the Pt 4f emission and no change in its binding energy occurs. Pt therefore remains in its metallic state. No formation of Pt oxides is observed.[48] For a BST film thickness >2 nm, the line shapes of the BST emissions are identical to those of the thick film.

D. Barrier heights

The Fermi level position in $SrTiO_3$:Nb or in the $(Ba,Sr)TiO_3$ layer at the interface determines the Schottky barrier height. X-ray excited valence band spectra of the $SrTiO_3$ substrate as well as of the $(Ba,Sr)TiO_3$ substrate and overlayer are presented in Fig. 5. The valence band maxima of the $SrTiO_3$:Nb crystal and the $(Ba,Sr)TiO_3$ films are determined by linear extrapolation of the leading edge of the valence band emission with an uncertainty of ±0.1 eV. The VBM is at $E_F - E_{VB} = 3.25$ eV for the $SrTiO_3$:Nb surface, 2.4 eV for the ~200 nm thick $Ba_{0.6}Sr_{0.4}TiO_3$ film used as substrate for the deposition of Pt, and 2.2 eV for the ~20 nm thick $(Ba,Sr)TiO_3$ film stepwise deposited onto Pt in the interface experiment, as described in Sec. III C

The evolution of substrate core level binding energies in the course of deposition is displayed in Fig. 6. Core level to valence band maximum binding energy differences were subtracted for better comparison. For deposition of Pt onto $(Ba,Sr)TiO_3$ (top graph in Fig. 6), the valence band maxima of the uncovered substrates correspond to the values derived from Figs. 5(a) and 5(b). The data from an additional experi-

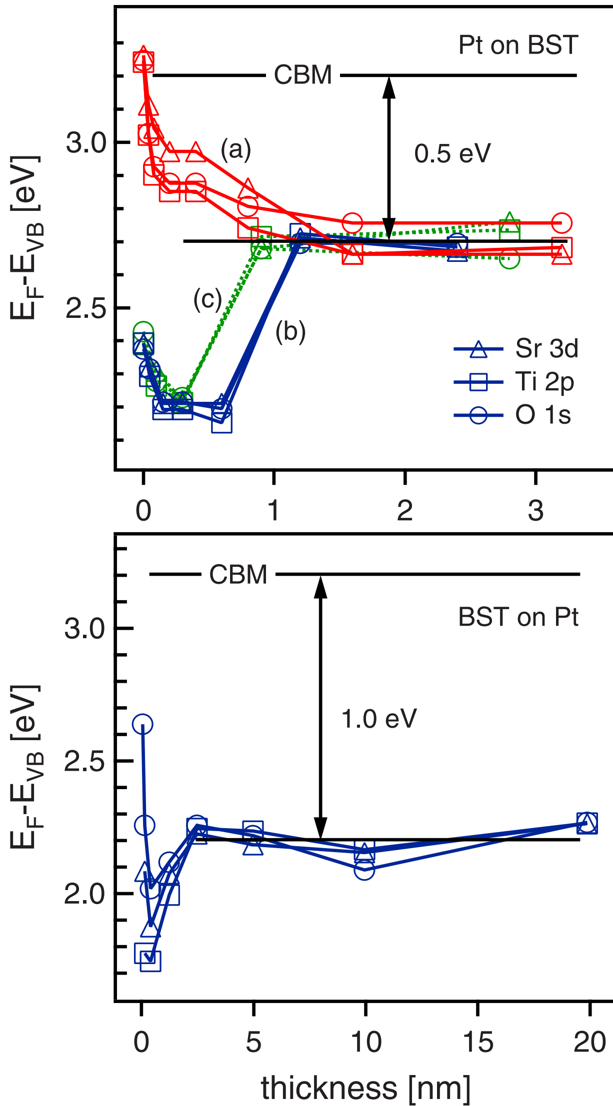

FIG. 6. (Color online) Evolution of $SrTiO_3$:Nb and $Ba_{0.6}Sr_{0.4}TiO_3$ valence band maximum binding energy with increasing film thickness for deposition of Pt onto BST (top) and for deposition of BST onto Pt (bottom). In the top graph, the three different experiments are (a) for single crystal $SrTiO_3$, (b) for stoichiometric, and (c) for nonstoichiometric $Ba_{0.6}Sr_{0.4}TiO_3$.

ment, wherein Pt has been deposited onto a nonstoichiometric substrate with a 10%–20% Ti excess, have been added for comparison.[49] For the deposition of $Ba_{0.6}Sr_{0.4}TiO_3$ onto Pt, the valence band maximum after growth of a ~20 nm thick film corresponds to the value derived from Fig. 5(c).

For all of the experiments shown in Fig. 6, there is a parallel shift of the core levels with increasing film thickness. This also indicates the absence of strong interface reactions. In the case of Pt deposition, a saturation of the binding energy shifts at $E_F - E_{VB} = 2.7 \pm 0.1$ eV for a Pt film thickness of ≥ 1 nm is observed for all of the three substrates. Together with the band gap of 3.2 eV, this corresponds to a Schottky barrier height for electrons of 0.5 ± 0.1 eV, which is in good agreement with the values reported in literature for comparable experiments.[20,21]

In the case of $Ba_{0.6}Sr_{0.4}TiO_3$ deposition, the binding energy shifts saturate for a film thickness ≥ 2 nm at $E_F - E_{VB} = 2.2 \pm 0.1$ eV. The Schottky barrier height for electrons then amounts to $\Phi_B = 1.0 \pm 0.15$ eV. For a $Ba_{0.6}Sr_{0.4}TiO_3$ film thickness <2 nm, the binding energies of the substrate do not exhibit parallel shifts, which is attributed to the yet incomplete development of the electronic structure of the material.

According to Fig. 6, the barrier heights obtained during deposition of Pt onto BST are significantly smaller than those obtained during deposition of BST onto Pt. This can cause the asymmetry in electrical behavior, which is observed in Pt/BST/Pt thin film capacitors.[11,50] As will be shown in the following, the asymmetry of the barrier heights is explained by the different preparation conditions of the respective interfaces. The deposition of Pt onto BST corresponds to reducing conditions, while more oxidizing conditions are present during deposition of BST onto Pt.

IV. VARIATION IN BARRIER HEIGHT WITH ANNEALING

A. Experimental results

X-ray photoelectron spectra of a $SrTiO_3$:Nb single crystal after different preparation steps are shown in Fig. 7. The spectra recorded from the uncovered single crystal surface and after deposition of ~2 nm of Pt agree well with those presented above. The valence band maximum energy for this particular sample is given by $E_F - E_{VB} = 3.1 \pm 0.05$ eV. After deposition of 2 nm of Pt, the substrate core levels are strongly attenuated and shifted by 0.5 ± 0.05 eV to a lower binding energy. The Schottky barrier height for electrons, which is given by the energy difference between the conduction band minimum E_{CB} and the Fermi level at the interface, then amounts to $\Phi_B = 0.6 \pm 0.1$ eV. The Fermi energy of the Pt film coincides with the independently calibrated zero of binding energy and the binding energy of the Pt $4f$ level amounts to 71.0 ± 0.05 eV.

After annealing of the sample in an oxygen atmosphere, the substrate emission lines have strongly increased in intensity and the intensity of the Pt $4f$ level is decreased. This is explained by the formation of three-dimensional islands of the Pt film, which forms a closed layer with a homogeneous thickness right after deposition (see Sec. III A). A comparable effect is also observed after annealing of the $(Ba,Sr)TiO_3$/Pt sample (compare Fig. 8). The morphology of the Pt film is indicated at the right of Fig. 7.

The substrate emission lines are all shifted to higher binding energies by ~0.1 eV, corresponding to a valence band maximum binding energy with respect to the Fermi energy of the substrate of $E_F - E_{VB} = 2.7$ eV. In addition, strong binding energy shifts are observed for the Pt emissions. The Pt $4f$ line is shifted by 0.8 eV and the Fermi edge by 0.7 eV to higher binding energies. There are no significant changes of the spectral shape of the Pt $4f$ and the valence band after annealing. This observation together with the reversibility of the binding energy shifts after annealing in vacuum (see below) indicates that the changes are not associated with chemical changes in Pt, e.g., to the formation of Pt oxide,[48] diffusion of Pt into the substrate or re-evaporation of Pt. The

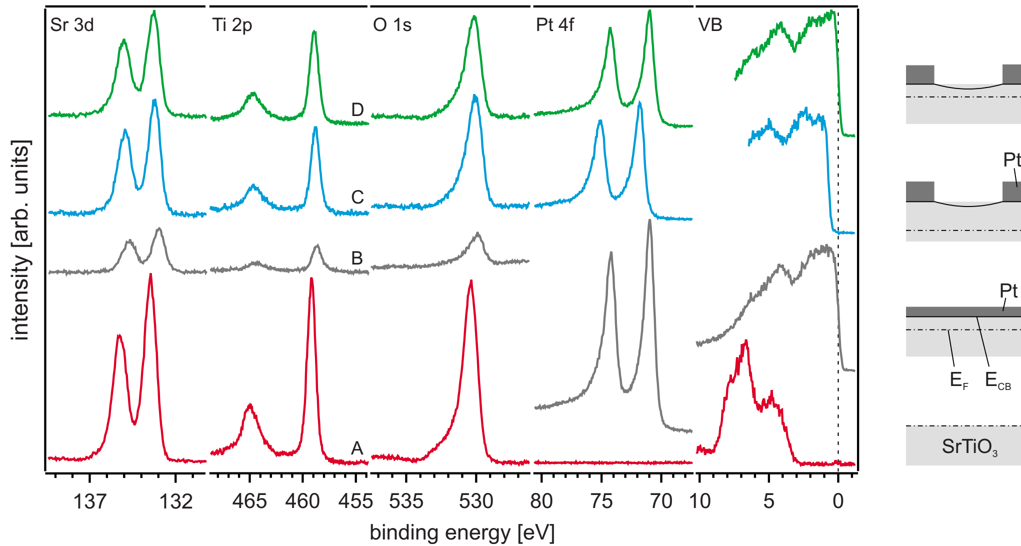

FIG. 7. (Color online) Photoelectron core level and valence band spectra of a $SrTiO_3$:Nb(100) single crystal after (a) heat treatment in 0.05 Pa oxygen pressure at 650 °C for 30 min, (b) deposition of 2 nm Pt, (c) subsequent annealing in 0.05 Pa oxygen pressure at 400 °C for 30 min, and (d) after subsequent annealing in vacuum (10^{-5} Pa) at 400 °C for 30 min. All of the spectra were recorded by using monochromatic Al $K\alpha$ radiation and referenced to the Fermi edge of a sputter cleaned Ag sample. The valence band spectra are normalized to the same intensity for better comparison. The morphology of the sample and the electronic structure is indicated on the right.

shifts of the Pt emission can be well explained by a surface photovoltage induced by the x-ray source, which can occur in such experiments.[51–54] The magnitude of the photovoltage corresponds well with the barrier height (see Sec. IV B).

A photovoltage leads to a shift of the Fermi level at the surface. This has to be added to the Fermi level of the substrate, which provides the reference binding energy in XPS, for a proper determination of the barrier height. After annealing in oxygen, the barrier height is then calculated as $\Phi_B = 1.2$ eV. As discussed below, this is only a lower boundary for the barrier height due to the influence of lateral inhomogeneous surface potentials, which leads to incomplete band bending in the regions between the Pt islands (see also the sketch of surface potential at the right part of Fig. 7).[53,54]

The topmost spectra in Fig. 7 were recorded after an additional annealing at 400 °C in vacuum for 30 min. No further changes in intensities compared to the previous annealing in 0.05 Pa oxygen pressure are observed. The Pt 4f and

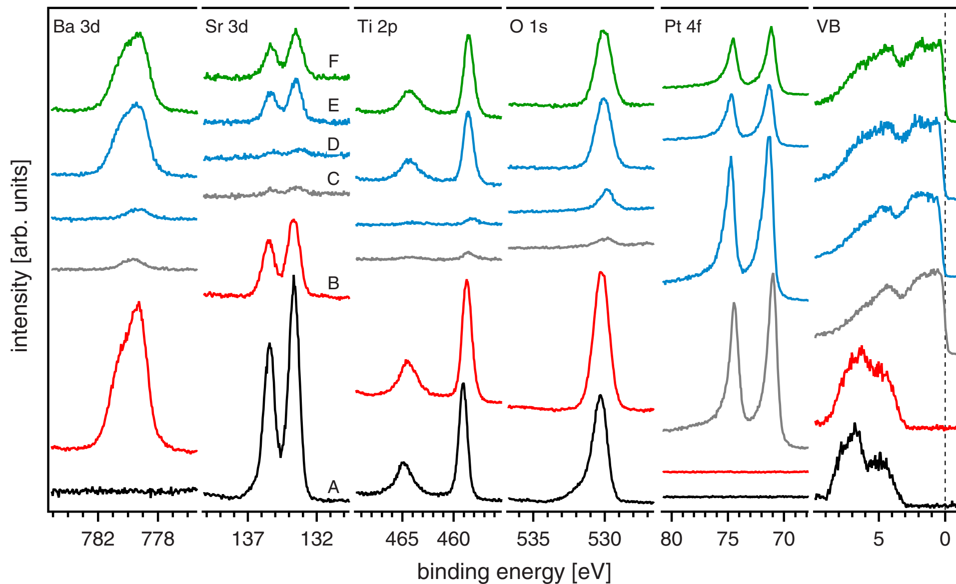

FIG. 8. (Color online) Photoelectron core level and valence band spectra of a $Ba_{0.6}Sr_{0.4}TiO_3$ thin film after (a) heat treatment in 0.05 Pa oxygen pressure at 650 °C for 30 min, (b) deposition of ~200 nm $Ba_{0.6}Sr_{0.4}TiO_3$ at 650 °C, (c) deposition of ~3 nm Pt, (d) annealing in 0.05 Pa oxygen pressure at 400 °C for 30 min, (e) annealing in 0.05 Pa oxygen pressure at 600 °C for 30 min, and (f) annealing in vacuum (10^{-5} Pa) at 400 °C for 30 min. All of the spectra were recorded by using monochromatic Al $K\alpha$ radiation and referenced to the Fermi edge of a sputter cleaned Ag sample. The valence band spectra are normalized to the same intensity for better comparison.

the Fermi edge emission are shifted back to the values for metallic Pt, indicating the absence of photovoltage. All of the substrate core level emissions are shifted to higher binding energies, resulting in a valence band maximum position of $E_F - E_{VB} = 2.9 \pm 0.1$ eV. Obviously, the vacuum annealing has lead to a strong decrease in the barrier height. The barrier height calculated from the substrate binding energies is only 0.3 eV, which is smaller than the barrier observed after Pt deposition. The difference might again be related to lateral inhomogeneities of the surface potential. The barrier height after vacuum anneal is thus comparable to the barrier height observed after Pt deposition.

A variation in the barrier height with annealing is also observed for interfaces of Pt with $(Ba,Sr)TiO_3$ thin films. In the corresponding experiment (Fig. 8), ~3 nm of Pt was deposited onto a ~200 nm thick $Ba_{0.6}Sr_{0.4}TiO_3$ film on a $SrTiO_3(100)$:Nb substrate. The $SrTiO_3$:Nb substrate was chosen to avoid photovoltage contributions from the bottom contact. No changes in intensity are observed after annealing in 0.05 Pa oxygen pressure at 400 °C but after annealing at 600 °C. The higher temperature needed to induce island formation compared to the temperature in the experiment discussed above is attributed to the thicker Pt film.

There are noticeable changes in the Ba 3*d* line shape during the experiment. The spectrum of the clean $Ba_{0.6}Sr_{0.4}TiO_3$ surface exhibits the known structure with a high binding energy surface component.[55] The splitting between the two components disappears with increasing Pt deposition as also observed by Li *et al.*[31] during Pt deposition onto $BaTiO_3$. After island formation (spectra E in Fig. 8), the Ba 3*d* surface component reappears, indicating that an uncovered $(Ba,Sr)TiO_3$ surface is exposed. The changes in Ba 3*d* line shape are, hence, also consistent with island formation of the Pt film. The binding energy shifts observed for the $Ba_{0.6}Sr_{0.4}TiO_3$ sample are smaller compared to those for the single crystal sample. After deposition of Pt the barrier height amounts to $\Phi_B = 0.5$ eV, which is in good agreement with the results described above.

A photovoltage is evident from the shifted Fermi edge and Pt 4*f* level after annealing in oxygen atmosphere. Again, the photovoltage disappeared after annealing in vacuum. After annealing in 0.05 Pa O_2 at 400 °C, the photovoltage amounts to 0.3 V and the barrier height is calculated to be 1.0 eV, which is the same as the one determined during deposition of $(Ba,Sr)TiO_3$ onto Pt. As island formation has not yet occurred after annealing at 400 °C, the corresponding barrier height is not affected by an inhomogeneous surface potential, which is also the case for deposition of $(Ba,Sr)TiO_3$ onto Pt (see Sec. III C). The agreement between both barrier heights therefore indicates that the large barrier obtained for deposition of $(Ba,Sr)TiO_3$ onto Pt is a result of the oxygen atmosphere that was present during deposition. The smaller photovoltage compared to the single crystal interface is related to the smaller barrier height (see Sec. IV B). The smaller barrier at the oxygen annealed $(Ba,Sr)TiO_3$/Pt interface (1.0 eV) compared to that at the oxygen annealed $SrTiO_3$:Nb/Pt interface (>1.2 eV) might be related to the polycrystalline nature of the film. An influence of the Ba content on the barrier height is also possible.

After annealing in 0.05 Pa O_2 at 600 °C, the photovoltage still amounts to 0.3 V, but the apparent barrier height is reduced to 0.7 eV. The identical photovoltage confirms that the barrier height under the Pt islands has not changed, as a reduction in barrier height would directly lead to a reduction in the photovoltage. Furthermore, this is clear evidence for the presence of lateral inhomogeneous surface potentials as origin for the change of substrate binding energies after island formation.

After annealing in vacuum, the photovoltage is reduced to 0.1 V, indicating a strong reduction in the barrier height. The calculated barrier height amounts to 0.5 eV. This is larger compared to that for the situation after annealing of the $SrTiO_3$:Nb/Pt interface. The annealing conditions might not have been sufficient to fully reduce the interface, as also indicated by the small but nonvanishing photovoltage.

B. Magnitude of the photovoltage

The photovoltage U_{ph} induced by x-ray source can be estimated by using

$$U_{ph} = \frac{k_B T}{q} \ln\left(\frac{j_{ph}}{j_0} + 1\right), \tag{1}$$

where k_B is Boltzmann's constant, T is the temperature, q is the elementary charge, j_{ph} is the photocurrent density, and

$$j_0 = A^* T^2 \exp\left(-\frac{\Phi_B}{k_B T}\right) \tag{2}$$

is the reverse saturation current density for conduction by thermionic emission over the barrier.

The photon flux of the monochromated x-ray source ($h\nu = 1486.6$ eV) is $\sim 10^{11}$ photons/s (Ref. 56) and the illuminated area is estimated as ~2–4 mm^2. Assuming further that the energy required for the creation of an electron-hole pair is given on the average by $3 \times E_g$,[52] the photocurrent density induced by the x-ray source is calculated as ~1 mA/cm^2. With a barrier height of $\Phi_B = 1.2$ eV, this results in a photovoltage of $U_{ph} = 600$ meV, which is in very good agreement with the experimental value of 700 meV.

The small difference between the calculated and the experimental photovoltage can be related to an underestimation of the barrier height in the experiment due to the islands structure of the Pt film.[53,54] When the surface is only partially covered by the metal, the surface potential laterally becomes inhomogeneous (see Fig. 7). The magnitude of the lateral variation of the surface potential depends on the doping of the substrate and the distance between the Pt islands.[57] With Pt islands on the surface, the substrate signal mainly originates from the regions between the islands. As a larger band bending occurs under the Pt islands, the barrier height is consequently underestimated when derived from the substrate binding energies. By using a slightly larger barrier height of 1.3 eV, the photovoltage is calculated to 700 meV, exactly reproducing the experimental value. This agreement might be to some extent fortuitous due to the uncertainties in the calculation. Even larger barrier heights are therefore possible. In any case, the agreement between experimental and calculated photovoltage provides additional evidence that the observed shifts of the Pt emissions after the oxygen anneal-

ing are related to a photovoltage induced by the x-ray source. Consequently, by taking into account the uncertainty in the lateral variation of the surface potential, the Schottky barrier height after oxygen annealing is $\Phi_B \geq 1.2$ eV for the single crystal $SrTiO_3$:Nb/Pt. In principle, a temperature dependent study of the photovoltage could reveal more details of the transport properties and allow for an independent determination of the barrier height.[53,54]

The photovoltage calculated for a barrier height of $\Phi_B = 0.6$ eV amounts to 20 mV when using the same parameters as above. This justifies that no detectable x-ray source induced photovoltage has to be expected for the as prepared and the vacuum annealed interfaces, which is in agreement with the experimental observations.

C. Barrier heights

Apparently, there are two different states of the interface, which result in different barrier heights. The as-deposited and the vacuum annealed interfaces can be regarded as the *reduced state* of the interface with a barrier height of $\Phi_B = 0.5 \pm 0.1$ eV. The oxygen annealed interface can be regarded as the *oxidized state* of the interface with a barrier height of $\Phi_B \geq 1.2$ eV for single crystal $SrTiO_3$ and of 1.0 eV for polycrystalline $(Ba,Sr)TiO_3$.

Although several authors have reported a dependence of the Schottky barrier height on atmosphere,[6,17,18] so far only Dawber *et al.*[3,24] presented an explanation for this observation. They used the model of Cowley and Sze[25] to calculate the Schottky barrier height. This model is a phenomenological approach to describe the variation in Schottky barrier height with metal work function and the degree of Fermi level pinning.[58] In addition to the semiconductor space charge and the charge in the metal, it phenomenologically introduces semiconductor interfaces states. The charge in the interface states is determined by the relative position of the Fermi level with respect to the *charge neutrality level* (E_{CNL}), which is associated with the interface states. The position of the charge neutrality level is related to the electronic band structure of the semiconductor and was calculated by Robertson and Chen[22] for $SrTiO_3$ as $\phi_0 = E_{CNL} - E_{VB} = 2.6$ eV above the valence band maximum.

In the model of Cowley and Sze,[25] the barrier height for electrons is given by

$$\Phi_B = [S(\phi_m - \chi) + (1-S)(E_g - \phi_0) - \Delta\Phi] + \left\{ \frac{S^2 C}{2} - S^{3/2} \cdot \left[C(\phi_m - \chi) + (1-S)(E_g - \phi_0)\frac{C}{S} - \frac{C}{S}(\xi - k_B T) + \frac{C^2 S}{4} \right]^{1/2} \right\}, \quad (3)$$

where ϕ_m is the metal work function, χ is the semiconductor electron affinity, $\Delta\Phi$ is the image force Schottky barrier lowering, and $\xi = E_{CB} - E_F$ is the Fermi level position in the bulk of the semiconductor. The two parameters S and C are given by

$$S = \frac{\varepsilon_i}{\varepsilon_i + q d_i N_i}, \quad C = \frac{2 q \varepsilon_s N_D d_i^2}{\varepsilon_i^2}. \quad (4)$$

where ε_i and ε_s are the interface and bulk dielectric permittivity, d_i is the thickness of the interface layer separating the interface states of the semiconductor from the surface charge of the metal, N_D is the bulk doping density, and N_i is the density of the semiconductor gap states. The index of interface behavior S can have values between 0 and 1 and describes the variation in the barrier height with metal work function. Low values of S are typically observed for covalent semiconductors as Si, Ge, and the III-V compounds[22,25,27,58,59] and indicate a strong Fermi level pinning (small variation in barrier height with metal work function) due to a high density of interface states.

First of all, interface states result from the wave function matching at the boundary and are therefore *intrinsic* even to crystallographically perfect interfaces. These states are commonly known as *metal-induced gap states*.[26,27,60,61] For semiconductors, which show a large Fermi level pinning, their density is on the order of 5×10^{14}/eV cm^2. In addition, *extrinsic interface states*, which arise from crystallographic defects, can also contribute to the interface charge density and therefore modify the barrier height. According to Eq. (3), a variation in the Schottky barrier can occur due to (i) a variation in the density of interface states N_i, (ii) a variation in the charge neutrality level, and (iii) a variation in doping. The latter is a result of the $\{\cdots\}$ term in Eq. (3), as emphasized by Dawber *et al.*[3,24]

Barrier heights calculated in dependence on bulk doping by using $\phi_0 = 2.6$ eV and the density of interface states as a parameter are shown in Fig. 9. At high doping levels, the barrier height decreases to zero, which is independent on the density of interface states. This is due to the increase in space charge density with increased doping and mathematically expressed by the $\{\cdots\}$ term in Eq. (3). The larger the doping is, the smaller is the band bending that can develop. Hence, in the high doping limit, the Fermi level position at the interface should approach the Fermi level position in the bulk. As the free electron concentration in Nb-doped $SrTiO_3$ approximately equals the Nb content,[38] it is reasonable to assume that Nb is a shallow donor level in $SrTiO_3$. For electron concentrations of $\sim 10^{19}$ cm^{-3}, the bulk Fermi level should then be near the conduction band minimum or even inside the conduction band as for degenerate semiconductors[58] and as observed for the uncovered $SrTiO_3$:Nb substrate (see Fig. 5). Consequently, the barrier height for electrons should vanish in the high doping limit, as represented by the curves in Fig. 9.

A Nb content of 0.05 wt % in $SrTiO_3$ corresponds to a dopant concentration of $1.7 \cdot 10^{19}$ cm^{-3}. According to Fig. 9, a barrier height of ~ 0.5 eV is only possible for a very high concentration of interface defects. For this case, no variation of the barrier height with doping is expected. A variation will only be observed by a change in defect concentration. However, the barrier height should then vary between 0 and ~ 0.5 eV (see arrow "A" in Fig. 9) and not between 0.5 and 1.2 eV, as observed in the current experiment and reported in literature.[6,17,18]

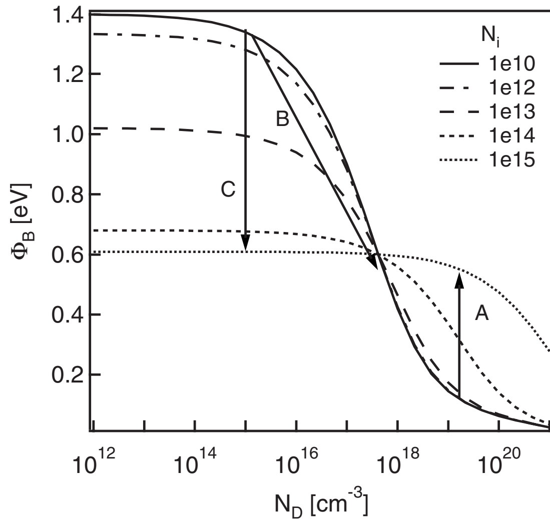

FIG. 9. Schottky barrier heights in dependence on the doping level N_D of $SrTiO_3$ as calculated from Eq. (3) for different densities of interface states N_i. The values inserted for $\phi_0=2.6$ eV, $d_i=0.5$ nm, $\varepsilon_s=400\varepsilon_0$, and $\varepsilon_i=\varepsilon_0$ are the same as those used by Dawber and Scott (Refs. 3 and 24). For the Pt work function and the $SrTiO_3$ electron affinity, we have used the values of $\phi_m=5.6$ eV and $\chi=4.2$ eV, respectively. The density of interface states N_i is used as a parameter. The arrows indicate the possible variation in barrier height with changes in doping or defect concentration as discussed in the text.

Following Fig. 9, a variation in the barrier height between 0.5 and 1.2 eV can occur by a change in doping for a low concentration of interface defects (arrow "B" in Fig. 9) or for a change in interface defect concentration for a doping level $N_D < 10^{17}$ cm^{-3} (arrow "C" in Fig. 9). In principle, a change in doping might occur during annealing by a change in stoichiometry, which is related, e.g., to a change in oxygen vacancy concentration in a region near the surface. However, in Nb-doped $SrTiO_3$, oxygen vacancies are minor defect species and a change in doping would therefore only be possible by diffusion of either Nb or Sr.[62] Neither is likely at a temperature of only 400 °C. Hence, it is concluded that a change in defect concentration at the interface is responsible for the change in barrier height.

An additional experiment was carried out in which a 1 nm thick Pt layer was first deposited onto a cleaned $SrTiO_3$ surface. Subsequently, the sample was annealed at 400 °C in 0.05 Pa oxygen pressure for 30 min. The observed binding energies, and thus, the barrier height agree with those described in Sec. IV A. After the oxygen annealing, which also resulted in a strong decrease in the Pt signal and an increase in the substrate signals, stepwise Pt deposition was continued. In the course of the subsequent Pt deposition, the x-ray source induced photovoltage disappeared again and the binding energies correspond to a barrier height of $\Phi_B=0.4$ eV. The deposition of Pt was carried out at room temperature, at which bulk diffusion can be neglected. The observed changes can therefore not be explained by a change in doping and therefore confirm that a change of interfacial defect concentration is responsible for the change in the barrier height.

The attribution of the origin of the change in the barrier height to changes in interface defect concentration does not exclude that doping has an effect on the barrier. Gopalan *et al.*[16] reported a variation in barrier height with doping. Φ_B reduces from 1.3 eV for undoped $SrTiO_3$ to 1 and 0.9 eV for $SrTiO_3$ doped with 1.7×10^{20} and 8.4×10^{20} cm^{-3} niobium. Only a small reduction (<0.1 eV) in the barrier height is observed by the authors for $SrTiO_3$ doped with 1.7×10^{19} cm^{-3} Nb, which is the doping level also used in the present experiment.

The effect of doping on the barrier height is, however, much smaller than expected from Eq. (3) and Fig. 9. In addition, the observed barrier heights can only be understood if the effective doping concentration in the space charge region is considerably smaller than the nominal Nb concentration, which is the effective dopant concentration in the bulk and determines the electron concentration in transport studies.[38] This behavior is not understood yet. However, it has also not been possible to measure the resistance of the crystals by using a mechanical contact with conventional multimeter tips, despite the high conductivity of the crystals. This observation also suggests a rather insulating surface layer.

V. ORIGIN OF INTERFACIAL DEFECT STATES

Based on the results described in Sec. IV, it is concluded that the variation in barrier height with annealing is due to changes in the defect concentration at the interface. In principle, this can be due to a different *intrinsic* defect concentration as a result of the atomic arrangement at the interface as, e.g., at Si/silicide interfaces (see Ref. 63 and references therein). In this section, we provide evidence that the concentration of *extrinsic* surface states varies between the oxidized and the reduced state of the interface.

The defects, which lead to a low barrier height of $\Phi_B=0.5\pm0.1$ eV, are created either by deposition of Pt or by annealing in a reducing atmosphere. Defect formation by deposition of Pt can occur even if a chemical reaction between Pt and the substrate is thermodynamically not possible. Rao *et al.*[23] calculated the binding energy of Pt on $BaTiO_3$ to be ~4 eV. This heat of condensation is released when Pt atoms are deposited onto a substrate and can lead to defect formation, as proposed by Spicer *et al.*[64] Such a defect formation has been observed, e.g., in the course of Pt evaporation onto chemically inert van der Waals surfaces of the layered semiconductor WSe_2.[65] It is remarked that the heat of condensation is larger than the average kinetic energy of the Pt atoms in the vapor phase, even in the case of sputter deposition.

The defect concentration is strongly reduced by annealing in oxygen atmosphere, which leads to a considerably larger Schottky barrier height of $\Phi_B\geq1.2$ eV. According to this, it is straightforward to associate the active defects at the interface with oxygen vacancies (V_O). Oxygen vacancies in $SrTiO_3$ are expected to form electronic states close to the conduction band[66,67] and can therefore indeed account for the observed lowering of Φ_B. As the charge of the oxygen vacancy is shared with the neighboring Ti atoms, the presence of oxygen vacancies might show up in the occurrence of reduced Ti species. These are indeed observed in our annealing experiments. Difference spectra of the Ti 2p levels re-

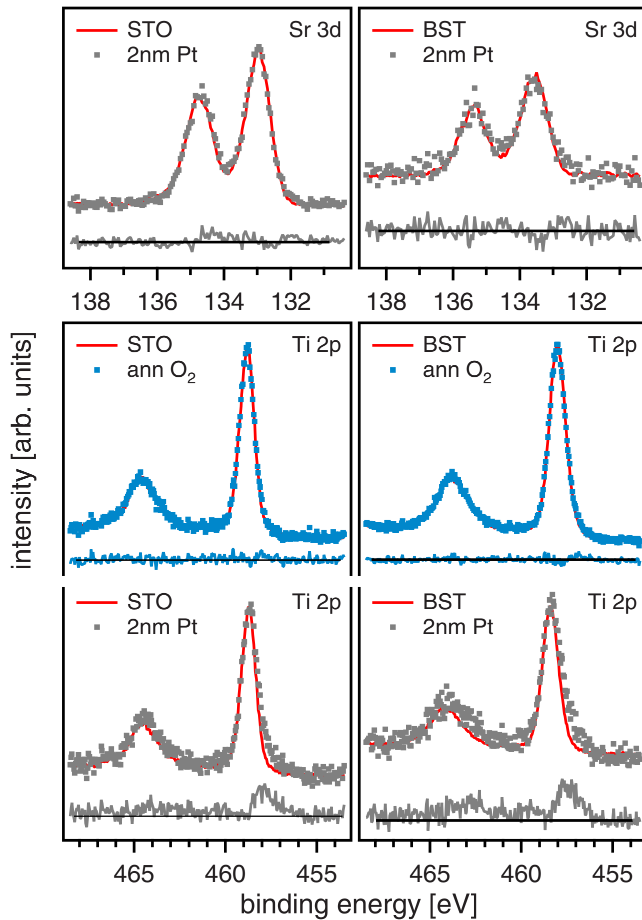

FIG. 10. (Color online) Left column: Ti 2p difference spectra between the clean single crystal $SrTiO_3$:Nb substrate and the sample covered with 2 nm of Pt (bottom) and between clean $SrTiO_3$:Nb and the Pt covered sample after annealing in oxygen (middle). The Sr 3d spectra of the clean and Pt covered sample are compared in the top graph. The spectra are normalized and shifted in energy. Right column: The same difference spectra for polycrystalline $Ba_{0.6}Sr_{0.4}TiO_3$.

corded during annealing of the $SrTiO_3$:Nb/Pt sample (Fig. 7) are presented in the left column of Fig. 10. Difference spectra from the data for the polycrystalline (Ba,Sr)TiO_3 substrate (Fig. 8) show comparable effects but are rather noisy due to the strong attenuation of the substrate levels after Pt deposition. Data from another experiment with a thinner Pt film are therefore included in Fig. 10 for comparison.

The Ti 2p spectra of the clean substrates show symmetric emission peaks. After Pt deposition a noticeable emission at the low binding energy side of the peak maximum occurs. After subsequent annealing in oxygen, again symmetric peaks are observed. The emission at 457–458 eV binding energy observed after Pt deposition can be attributed to the presence of reduced Ti^{3+} species.[68] The corresponding difference spectra of the Sr 3d emissions do not show an increased emission at lower binding energies comparable to the Ti 2p emission. It can therefore be ruled out that the additional emission in the Ti 2p peak is due to a lateral inhomogeneous Fermi level position. Hence, the spectra provide clear evidence for the presence of oxygen vacancies in the reduced state of the interface.

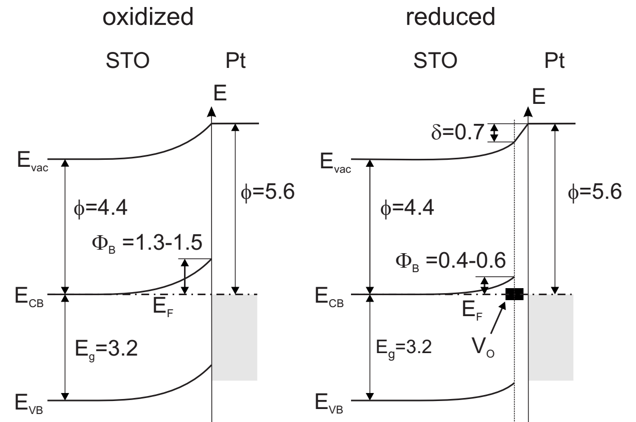

FIG. 11. Experimentally determined energy band diagrams for the $SrTiO_3$:Nb/Pt interface in the oxidized state without oxygen vacancies and the reduced state with oxygen vacancies. The barrier heights for the oxidized and reduced (Ba,Sr)TiO_3/Pt interface are 1.0 and 0.5 eV, respectively.

VI. SUMMARY AND CONCLUSIONS

The interface formation of $SrTiO_3$:Nb single crystals and (Ba,Sr)TiO_3 thin films with Pt has been studied by using photoelectron spectroscopy. The study reveals a direct determination of the barrier heights at the interface and their dependence on sample treatment and deposition sequence. In addition, the origin of the variation in the barrier height could be identified.

We observe no strong chemical interactions at the interfaces. A Schottky barrier height of $\Phi_B=0.5\pm0.1$ eV is obtained when Pt is deposited onto a clean (100) surface of a $SrTiO_3$:Nb single crystal or onto an *in situ* prepared polycrystalline (Ba,Sr)TiO_3 thin film. The deposition of Pt leads to the formation of oxygen vacancies, as indicated from the occurrence of reduced Ti species. The vacancy formation is attributed to the release of the heat of condensation of the Pt atoms.

The oxygen vacancies are removed after annealing of the $SrTiO_3$/Pt and (Ba,Sr)TiO_3/Pt interfaces in a low oxygen partial pressure of 0.05 Pa. At the same time, the Schottky barrier height increases to $\Phi_B\geq1.2$ eV for $SrTiO_3$:Nb/Pt and to 1.0 ± 0.1 eV for (Ba,Sr)TiO_3/Pt. Annealing in vacuum reduces the barrier height to the value directly obtained after deposition of Pt. The two different situations for the oxidized and reduced interface states are sketched in Fig. 11.

The uncertainty of the barrier height for the oxidized $SrTiO_3$/Pt interface is caused by the presence of Pt islands, which cause a lateral inhomogeneous potential distribution. The contribution of the lateral inhomogeneous potential has been explicitly shown for the (Ba,Sr)TiO_3/Pt interface, where a thicker Pt film did not lead to island formation during annealing at 400 °C for 30 min. For a correct determination of the barrier heights, the photovoltage induced by the

x-ray source during measurement must be taken into account.

Any theoretical calculation of the barrier height of the contact has to be compared to the experimental value for the oxidized state as long as no extrinsic interfacial defects are introduced in the calculation. The direct evaluation of the photoemission data gives only a lower limit of 1.2 eV. However, a larger value is likely due to the lateral inhomogeneous potential. A larger value is also indicated from a quantitative comparison of the source induced photovoltage to a calculation based on thermionic emission theory. Taking the maximum reported value for the barrier height from Table I, we state a barrier height for the defect-free interface of 1.3–1.5 eV. The value given by Robertson and Chen[22] (0.89 eV) is significantly smaller. This is partially related to their use of a smaller Pt work function of only 5.3 eV. However, due to the rather strong Fermi level pinning derived by Robertson and Chen[22] ($S=0.28$), taking the experimental Pt work function of 5.5–5.6 eV will not significantly alter this result.

The experimentally determined barrier height for the oxidized interface roughly amounts to the difference between the electron affinity of $SrTiO_3$ and the work function of Pt (see Fig. 11). This agreement is, however, considered as fortuitous as the electron affinity of $SrTiO_3$ significantly varies with surface preparation.[40,41]

The dependence of the barrier height on sample treatment explains the asymmetry of electrical properties and the increased leakage current of as-deposited Pt/BST/Pt thin film capacitors.[11,50] Due to the defect formation during Pt deposition, the potential distribution in such a capacitor is highly asymmetric as the bottom contact exhibits a large barrier of 1.0 eV, while the top contact has a small barrier of 0.5 eV. After oxidation, typically performed as a rapid thermal annealing in air, the barrier height at the top contact increases to 1.0 eV, thereby establishing a symmetric potential distribution. The situation is summarized in Fig. 12.

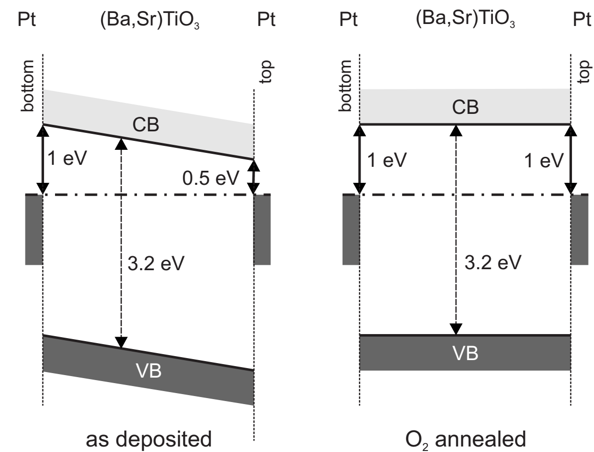

FIG. 12. Energy band diagrams for Pt/BST/Pt thin film capacitors with barrier heights derived from the presented experiments. A fully depleted (undoped) $(Ba,Sr)TiO_3$ layer is assumed for simplicity.

ACKNOWLEDGMENTS

This work was supported by the German Science Foundation within the research training group GRK 1037 (Tunable Integrated Components in Microwaves and Optics) and the European network of Excellence FAME. We further acknowledge discussions with R. de Souza from RWTH Aachen.

[1] *Nanoelectronics and Information Technology*, edited by R. Waser (Wiley-VCH, Weinheim, 2003).
[2] A. K. Tagantsev, V. O. Sherman, K. F. Astafiev, J. Venkatesh, and N. Setter, J. Electroceram. **11**, 5 (2003).
[3] M. Dawber, K. M. Rabe, and J. F. Scott, Rev. Mod. Phys. **77**, 1083 (2005).
[4] M. Cardona, Phys. Rev. **140**, A651 (1965).
[5] G. W. Dietz, W. Antpöhler, M. Klee, and R. Waser, J. Appl. Phys. **78**, 6113 (1995).
[6] J. D. Baniecki, R. B. Laibowitz, T. M. Shaw, K. L. Saenger, P. R. Duncombe, C. Cabral, D. E. Kotecki, H. Shen, J. Lian, and Q. Y. Ma, J. Eur. Ceram. Soc. **19**, 1457 (1999).
[7] R. Plonka, R. Dittmann, N. A. Pertsev, E. Vasco, and R. Waser, Appl. Phys. Lett. **86**, 202908 (2005).
[8] P. J. Schorn, D. Bräuhaus, U. Böttger, R. Waser, G. Beitel, N. Nagel, and R. Bruchhaus, J. Appl. Phys. **99**, 114104 (2006).
[9] O. Auciello, S. Saha, D. Y. Kaufman, S. K. Streiffer, W. Fan, B. Kabius, J. Im, and P. Baumann, J. Electroceram. **12**, 119 (2004).
[10] G. W. Dietz, M. Schumacher, R. Waser, S. K. Streiffer, C. Basceri, and A. I. Kingon, J. Appl. Phys. **82**, 2359 (1997).
[11] J. T. Li and X. L. Dong, Mater. Lett. **59**, 2863 (2005).
[12] K. Abe and S. Komatsu, Jpn. J. Appl. Phys., Part 1 **31**, 2985 (1992).
[13] K. H. Ahn, S. Baik, and S. S. Kim, J. Appl. Phys. **92**, 2651 (2002).
[14] Y. Fukuda, K. Numata, K. Aoki, A. Nishimura, G. Fujihashi, S. Okamura, S. Ando, and T. Tsukamoto, Jpn. J. Appl. Phys., Part 2 **37**, L453 (1998).
[15] C. S. Hwang *et al.*, J. Appl. Phys. **83**, 3703 (1998).
[16] S. Gopalan, V. Balu, J.-H. Lee, J. Hee-Han, and J. C. Lee, Appl. Phys. Lett. **77**, 1526 (2000).
[17] R. Liedtke, M. Grossmann, and R. Waser, Appl. Phys. Lett. **77**, 2045 (2000).
[18] N. Cramer, A. A. Mahmud, and T. S. Kalkur, Appl. Phys. Lett. **87**, 032903 (2005).
[19] D. Y. Wang, J. Am. Ceram. Soc. **77**, 897 (1994).
[20] M. Copel, P. R. Duncombe, D. A. Neumayer, T. M. Shaw, and R. M. Tromp, Appl. Phys. Lett. **70**, 3227 (1997).
[21] Y. W. Chung and W. B. Weissbard, Phys. Rev. B **20**, 3456 (1979).
[22] J. Robertson and C. W. Chen, Appl. Phys. Lett. **74**, 1168 (1999).
[23] F. Rao, M. Kim, A. J. Freeman, S. Tang, and M. Anthony, Phys. Rev. B **55**, 13953 (1997).
[24] M. Dawber, J. F. Scott, and A. J. Hartmann, J. Eur. Ceram. Soc. **21**, 1633 (2001).
[25] A. M. Cowley and S. M. Sze, J. Appl. Phys. **36**, 3212 (1965).

[26] J. Tersoff, Phys. Rev. Lett. **52**, 465 (1984).
[27] W. Mönch, *Electronic Properties of Semiconductor Interfaces* (Springer-Verlag, Heidelberg, 2003).
[28] P. Erhart, K. Albe, and A. Klein, Phys. Rev. B **73**, 205203 (2006).
[29] See, e.g., the Conference Records of the International Conference on Physics and Chemistry of Semiconductor Interfaces (PCSI) (unpublished).
[30] R.-V. Wang and P. C. McIntyre, J. Appl. Phys. **94**, 1926 (2003).
[31] X. L. Li, B. Chen, H. Y. Jing, H. B. Lu, B. R. Zhao, Z. H. Mai, and Q. J. Jia, Appl. Phys. Lett. **87**, 222905 (2005).
[32] J. X. Liao, C. R. Yang, Z. Tian, H. G. Yang, and L. Jin, J. Phys. D **39**, 2473 (2006).
[33] B. Psiuk, J. Szade, H. Schroeder, H. Haselier, M. Mlynarczyk, R. Waser, and K. Szot, Appl. Phys. A: Mater. Sci. Process. **89**, 451 (2007).
[34] M. K. Bahl, S. C. Tsai, and Y. W. Chung, Phys. Rev. B **21**, 1344 (1980).
[35] D. Ensling, A. Thissen, Y. Gassenbauer, A. Klein, and W. Jaegermann, Adv. Eng. Mater. **7**, 945 (2005).
[36] H. P. R. Frederikse and W. R. Hosler, Phys. Rev. **161**, 822 (1967).
[37] O. N. Tufte and P. W. Chapman, Phys. Rev. **155**, 796 (1967).
[38] M. V. Rozhdestvenskaya, I. T. Sheftel', V. A. Stogova, M. S. Kozyreva, and E. K. Krayukhina, Sov. Phys. Solid State **12**, 674 (1970).
[39] R. Schafranek, A. Giere, A. G. Balogh, Th. Enz, Y. Zheng, P. Scheele, R. Jakoby, and A. Klein (unpublished).
[40] R. Schafranek and A. Klein, Solid State Ionics **177**, 1659 (2006).
[41] V. E. Henrich, G. Dresselhaus, and H. J. Zeiger, Phys. Rev. B **17**, 4908 (1978).
[42] *CRC Handbook of Chemistry and Physics*, 65th ed., edited by R. C. Weast (CRC, Boca Raton, 1985).
[43] A. Asthagiri and D. S. Sholl, Surf. Sci. **581**, 66 (2005).
[44] J. F. Moulder, W. F. Stickle, P. E. Sobol, and K. D. Bomben, *Handbook of X-Ray Photoelectron Spectroscopy* (Physical Electronics, Eden Prairie, 1995).
[45] G. K. Wertheim and S. B. DiCenzo, Phys. Rev. B **37**, 844 (1988).
[46] unpublished results.
[47] L.-G. Ekedahl, M. Eriksson, and I. Lundström, Acc. Chem. Res. **31**, 249 (1998).
[48] F. Parmigiani, E. Kay, and P. S. Bagus, J. Electron Spectrosc. Relat. Phenom. **50**, 39 (1990).
[49] J. Im, O. Auciello, P. K. Baumann, S. K. Streiffer, D. Y. Kaufman, and A. R. Krauss, Appl. Phys. Lett. **76**, 625 (2000).
[50] J. Im, S. K. Streiffer, O. Auciello, and A. R. Krauss, Appl. Phys. Lett. **77**, 2593 (2000).
[51] M. Alonso, R. Cimino, and K. Horn, Phys. Rev. Lett. **64**, 1947 (1990).
[52] M. H. Hecht, Phys. Rev. B **41**, 7918 (1990).
[53] R. Schlaf, A. Klein, C. Pettenkofer, and W. Jaegermann, Phys. Rev. B **48**, 14242 (1993).
[54] A. Klein, C. Pettenkofer, W. Jaegermann, M. C. Lux-Steiner, and E. Bucher, Surf. Sci. **321**, 19 (1994).
[55] J. D. Baniecki, M. Ishii, T. Shioga, K. Kurihara, and S. Miyahara, Appl. Phys. Lett. **89**, 162908 (2006).
[56] J. Moulder, Physical Electronics Inc, (private communication).
[57] K. E. Miyano, D. M. King, C. J. Spindt, T. Kendelewicz, R. Cao, Z. Yu, I. Lindau, and W. E. Spicer, Phys. Rev. B **43**, 11806 (1991).
[58] S. M. Sze, *Physics of Semiconductor Devices* (Wiley, New York, 1981).
[59] S. Kurtin, T. C. McGill, and C. A. Mead, Phys. Rev. Lett. **22**, 1433 (1969).
[60] V. Heine, Phys. Rev. **138**, A1689 (1965).
[61] S. G. Louie, J. R. Chelikowsky, and M. L. Cohen, Phys. Rev. B **15**, 2154 (1977).
[62] R. Meyer, R. Waser, J. Helmbold, and G. Borchardt, Phys. Rev. Lett. **90**, 105901 (2003).
[63] R. T. Tung, J. Vac. Sci. Technol. B **11**, 1546 (1993).
[64] W. E. Spicer, P. W. Chye, P. R. Skeath, C. Y. Su, and I. Lindau, J. Vac. Sci. Technol. **16**, 1422 (1979).
[65] A. Klein, C. Pettenkofer, W. Jaegermann, T. Chassé, K. Horn, M. C. Lux-Steiner, and E. Bucher, Surf. Sci. Lett. **264**, L193 (1992).
[66] J. Robertson, J. Appl. Phys. **93**, 1054 (2003).
[67] J. Carrasco, F. Illas, N. Lopez, E. A. Kotomin, Y. F. Zhukovskii, R. A. Evarestov, Y. A. Mastrikov, S. Piskunov, and J. Maier, Phys. Rev. B **73**, 064106 (2006).
[68] W. Göpel, G. Rocker, and R. Feierabend, Phys. Rev. B **28**, 3427 (1983).